JACS
JOURNAL OF THE AMERICAN CHEMICAL SOCIETY

Subscriber access provided by ISTANBUL TEKNIK UNIV

Article

Comparative Structural and Chemical Studies of Ferritin Cores with Gradual Removal of their Iron Contents

Natividad Ga#lvez, Bele#n Ferna#ndez, Purificacio#n Sa#nchez, Rafael Cuesta, Marcelo Ceoli#n, Miguel Clemente-Leo#n, Susana Trasobares, Miguel Lo#pez-Haro, Jose J. Calvino, Odile Ste#phan, and Jose# M. Domi#nguez-Vera

J. Am. Chem. Soc., **2008**, 130 (25), 8062-8068 • DOI: 10.1021/ja800492z • Publication Date (Web): 29 May 2008

Downloaded from http://pubs.acs.org on February 8, 2009

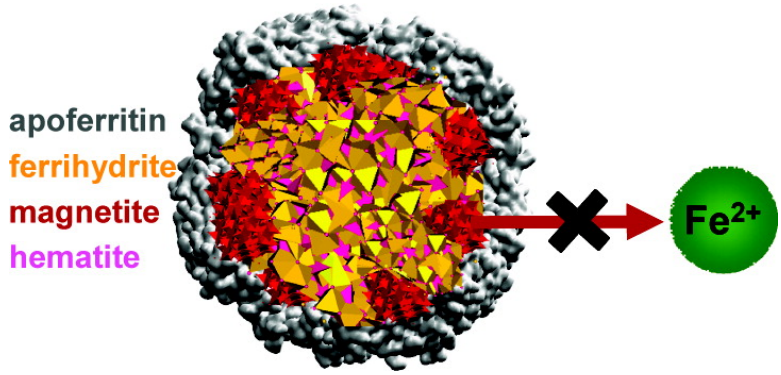

More About This Article

Additional resources and features associated with this article are available within the HTML version:

- Supporting Information
- Links to the 1 articles that cite this article, as of the time of this article download
- Access to high resolution figures
- Links to articles and content related to this article
- Copyright permission to reproduce figures and/or text from this article

View the Full Text HTML

ACS Publications
High quality. High impact.

Journal of the American Chemical Society is published by the American Chemical Society. 1155 Sixteenth Street N.W., Washington, DC 20036

J|A|C|S
ARTICLES

Published on Web 05/29/2008

Comparative Structural and Chemical Studies of Ferritin Cores with Gradual Removal of their Iron Contents

Natividad Gálvez,[†] Belén Fernández,[†] Purificación Sánchez,[†] Rafael Cuesta,[‡] Marcelo Ceolín,[*,§] Miguel Clemente-León,[||] Susana Trasobares,[⊥] Miguel López-Haro,[⊥] Jose J. Calvino,[⊥] Odile Stéphan,[#] and José M. Domínguez-Vera[*,†]

Departamento de Química Inorgánica, Universidad de Granada, 18071 Granada, Spain, Departamento de Química Inorgánica y Orgánica, EPS Linares, Universidad de Jaén, 23700 Linares, Spain, Instituto de Físico-Química Teórica y Aplicada, Universidad Nacional de La Plata, Argentina, Instituto de Ciencia Molecular, Universidad de Valencia, Fundació General de la Universitat de València (FGUV), Polígono de la Coma s/n, 46980 Paterna, Spain, Departamento Ciencia de Materiales e Ingeniería Metalúrgica y Química Inorgánica, Universidad de Cádiz, Campus Río San Pedro, 11510 Cádiz, Spain, and Laboratoire de Physiques des Solides, CNRS-UMR8502, Université Paris Sud, Bâtiment 510, 91405 Orsay, France

Received January 21, 2008; E-mail: josema@ugr.es

Abstract: Transmission Electron Microscopy (TEM), X-ray Absorption Near Edge Spectroscopy (XANES), Electron Energy-Loss Spectroscopy (EELS), Small-Angle X-ray Scattering (SAXS), and SQUID magnetic studies were performed in a batch of horse spleen ferritins from which iron had been gradually removed, yielding samples containing 2200, 1200, 500, and 200 iron atoms. Taken together, findings obtained demonstrate that the ferritin iron core consists of a polyphasic structure (ferrihydrite, magnetite, hematite) and that the proportion of phases is modified by iron removal. Thus, the relative amount of magnetite in ferritin containing 2200 to 200 iron atoms rose steadily from ~20% to ~70% whereas the percentage of ferrihydrite fell from ~60% to ~20%. These results indicate a ferrihydrite−magnetite core−shell structure. It was also found that the magnetite in the ferritin iron core is not a source of free toxic ferrous iron, as previously believed. Therefore, the presence of magnetite in the ferritin cores of patients with Alzheimer's disease is not a cause of their increased brain iron(II) concentration.

Introduction

Iron is an essential element for living organisms but is highly toxic in excess. The major intracellular storage form of iron is ferritin, a spherical protein composed of 24 subunits that surround an aqueous cavity capable of accommodating thousands of iron atoms (up to 4500) as an iron mineral, traditionally described as ferrihydrite.[1] Ferritin stores iron that is not required for immediate metabolic needs and at the same time protects against the toxic effects of its excess. Free intracellular iron catalyzes the production of oxygen free radicals via a Fenton reaction, which involves the reaction of hydrogen peroxide with iron(II) to produce the hydroxyl radical OH•, an extremely powerful oxidizing agent capable of causing extensive cell damage. Oxidative damage in neurons is known to be a primary cause of degenerative diseases such as Alzheimer's disease.[2]

Therefore, understanding the management of iron in the brain, especially the process of iron release from ferritin, is of great importance in the study of neurodegeneration. Once iron has been removed from ferritin, it is required for the activity of a number of cellular enzymes and pathways. Two experimentally established facts should be taken into account: (i) iron is accumulated in the brain in several neurodegenerative diseases,[3] and (ii) ferritin iron core composition significantly differs between physiological and pathological (especially Alzheimer's) brain ferritins.[4] Specifically, although both physiological and pathological ferritin cores have a polyphasic composition, the major phase is ferrihydrite (an iron(III) oxide) in physiological ferritin cores but mixed ferric−ferrous iron oxide (e.g., magnetite) in patients with Alzheimer's disease.[5] Considered together, this evidence suggests that ferritin dysfunction would

[†] Universidad de Granada.
[‡] Universidad de Jaén.
[§] Universidad Nacional de La Plata.
[||] Universidad de Valencia.
[⊥] Universidad de Cádiz.
[#] Université Paris Sud.

(1) (a) Chasteen, N. D.; Harrison, P. M. *J. Struct. Biol.* **1999**, *126*, 182–194. (b) Harrison, P. M.; Arosio, P. *Biochim. Biophys. Acta* **1996**, *1275*, 161–203. (c) Theil, E. C.; Takagi, H.; Small, G. W.; He, L.; Tripton, A. R.; Danger, D. *Inorg. Chim. Acta* **2000**, *297*, 242–251. (d) Liu, X.; Theil, E. C. *Acc. Chem. Res.* **2005**, *38*, 167–175.

(2) (a) Markesbery, W. R. *Free Radical Biol. Med.* **1997**, *23*, 134. (b) Perry, G.; Cash, A. D.; Smith, M. A. *J. Biomed. Biotechnol.* **2002**, *2*, 120–123.

(3) (a) Burdo, J. R.; Connor, J. R. *Biometals* **2003**, *16*, 63–75. (b) Ke, Y.; Qian, Z. M. *Lancet Neurol.* **2003**, 246–253.

(4) (a) Quintana, C.; Cowley, J. M.; Marhic, C. *J. Struct. Biol.* **2004**, *147*, 166–178. (b) Cowley, J. M.; Janney, D.; Gerkin, R. C.; Buseck, P. R. *J. Struc. Biol.* **2000**, *131*, 210–216.

(5) (a) Smith, M. A.; Harris, P. L. T.; Sayre, L. M.; Perry, G. *Proc. Natl. Acad. Sci. U.S.A.* **1997**, *94*, 9866–9868. (b) Moos, T.; Morgan, E. H. *Ann. N.Y. Acad. Sci.* **2004**, *1012*, 14–26.

10.1021/ja800492z CCC: $40.75 © **2008 American Chemical Society**

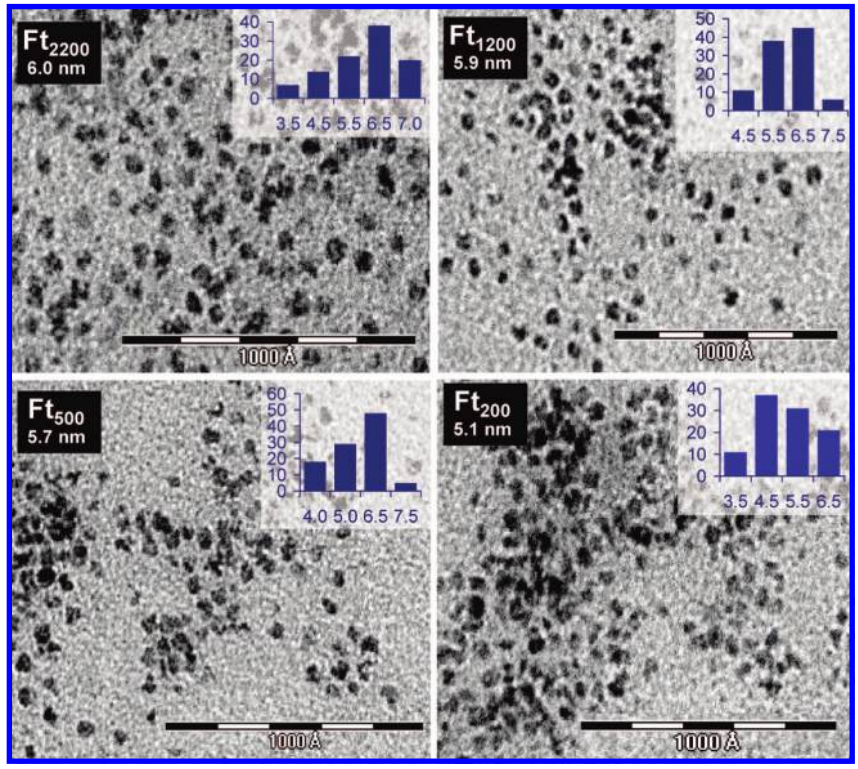

Figure 1. TEM micrographs of the ferritin samples Ft_{2200}, Ft_{1200}, Ft_{500}, and Ft_{200}, showing discrete electrodense iron cores. Scale bars are 100 nm. Inset: Particle size histograms (particle size vs freqency). Average particle size is indicated for each sample.

increase toxic brain ferrous ions, which may contribute to producing free radicals that induce the cellular oxidative stress associated with cognitive decline and Alzheimer's disease.[6]

Understanding the chemical structure of the ferritin core may help to elucidate the alteration or dysfunction of ferritin and its role in the development of degenerative diseases. Although the ferritin mineral core was traditionally described as ferrihydrite,[1] more recent studies have revealed a polyphasic structure, consisting of "classic" ferrihydrite and other phases, including a magnetite-like phase,[4,6] although the different phases do not coexist within the same core.

The present paper reports the study of ferritin core structure in a batch of horse spleen ferritins in which iron was gradually removed in a controlled manner[7] by the traditional procedure of reduction and iron(II) chelation, obtaining native ferritins containing 2200, 1200, 500, and 200 iron atoms. These samples (Ft_{2200}, Ft_{1200}, Ft_{500}, and Ft_{200}) served as a biomimetic model for studying the relationship between natural iron removal and iron core structure in brain ferritin.

Transmission Electron Microscopy (TEM), X-ray Absorption Near Edge Spectroscopy (XANES), Electron Energy-Loss Spectroscopy (EELS), Small-Angle X-ray Scattering (SAXS), and SQUID magnetic measurements demonstrated that the structure of ferritin iron core is formed by several iron oxide phases, which are modified in percentage terms as iron is gradually removed. Thus, our results show an increase in the magnetite phase with a corresponding decrease in the ferrihydrite phase. These techniques (TEM, XANES, EELS, SAXS, and SQUID measurements), more frequently used in Material Sciences than in Life Sciences, allowed us to clarify structural and chemical aspects of horse spleen ferritin under a process of gradual iron removal. Information obtained in this study can be used to solve the chemical composition of ferritin in pathological tissue samples and to interpret some properties, such as its NMR relaxometry. This technique could be a valuable tool for the diagnosis and follow-up of neurodegenerative diseases, as proposed by Brooks et al.[8]

We also found that the magnetite in ferritin is not a source of free ferrous ions for promoting the formation of OH• radicals, as widely believed.[9] Therefore, the presence of magnetite in the ferritin cores of patients with Alzheimer's disease is probably a consequence and not a cause of their increased brain iron(II) concentrations.

Results and Discussion

TEM Study. Figure 1 depicts TEM micrographs of ferritin samples with iron contents of 2200, 1200, 500, and 200 atoms. Tests on 100 ferritin particles from each sample showed that particle size did not decrease as expected for an iron removing surface mechanism. Thus, mean diameters (and standard deviations) were 6.0(0.7), 5.9(0.9), 5.7(1.0), and 5.1(1.0) nm for Ft_{2200}, Ft_{1200}, Ft_{500}, and Ft_{200}, respectively. Note that iron cores of the sample with the least iron content (Ft_{200}) are more irregular in shape and less electron dense compared with those of Ft_{1200} and Ft_{2000}.

One possible interpretation of the nonsignificant core size variation with iron removal is that some ferritin molecules lose

(6) Quintana, C. *Mini-Rev. Med. Chem.* **2007**, *7*, 961–975.
(7) Clemente-León, M.; Coronado, E.; Soriano-Portillo, A.; Colacio, E.; Domínguez-Vera, J. M.; Gálvez, N.; Madueño, R.; Martín-Romero, M. T. *Langmuir* **2006**, *22*, 6993–7000.
(8) (a) Vymazal, J.; Zak, O.; Bulte, J. W. M.; Aisen, P.; Brooks, R. A. *Magn. Reson. Med.* **1996**, *36*, 61–65. (b) Vymazal, J.; Brooks, R. A.; Patronas, N.; Hajek, M.; Bulte, J. W. M.; Di Chiro, G. *J. Neurosci.* **1995**, *134*, 19–26.
(9) Quintana, C. *J. Alzheimer's Dis.* **2007**, *12*, 157.

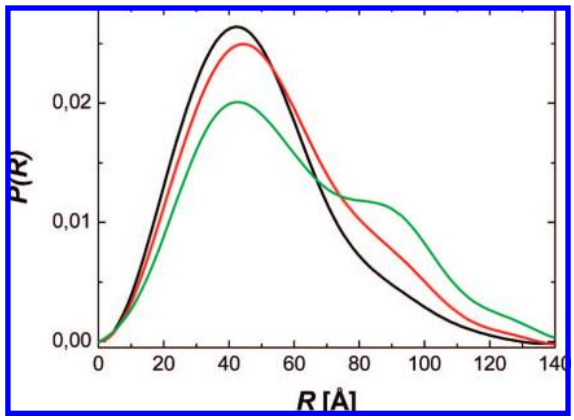

Figure 2. PDFs obtained from SAXS experiments after regularized Fourier Transform. Ft_{500} (green), Ft_{1200} (red), and Ft_{2200} (black)

all of their iron whereas others remain intact. However, this possibility can be ruled out, since negatively stained TEM images (Supporting Information) of all ferritin samples showed homogeneous metallic cores surrounded by apoferritin shells without the presence of empty apoferritin capsids.

Therefore, TEM results suggest that iron is removed from the center of the ferritin iron core, hollowing it out rather than reducing its size from the surface. Our observations contrast with the core diameters found (or calculated) for artificial horse spleen ferritins.[10] Thus, diameters of 5.6, 4.4, 3.9, and 2.8 nm were measured by TEM for synthesized ferritin containing 2000, 1000, 500, and 250 iron atoms, respectively. Another group that studied the apoferritin remineralization process reported diameters of 6.5 and 2.6 nm for cores with 2000 and 500 iron atoms.[11] Discrepancies between the present data and previous reports [9,10] reflect differences between ferritin cores obtained by artificially oxidative reconstitution of apoferritin and those obtained by iron removal reduction of native ferritin.

SAXS Study. Samples were studied by Small Angle X-ray Scattering. The method is based on the size and shape specificity of the scattering pattern of electromagnetic waves dispersed by electron density inhomogeneities in the sample. Figure 2 shows the PDFs (Pair Distribution Functions) obtained after regularized Fourier Transform of the scattering patterns obtained for Ft_{500}, Ft_{1200}, and Ft_{2200}.

Chemical reduction induced dramatic changes in the PDFs corresponding to the iron release process. Initially, little change was observed in the position of the first maximum at $R \approx 40$ Å, and there was no definite tendency. However, systematic reduction in the amplitude of the curve at $R \approx 40$ Å was accompanied by a simultaneous increase in the intensity at $R \approx 90$ Å. This behavior was also reflected in a shift in the mean R value from 44.3 Å in Ft_{2200} to 54.1 Å in Ft_{500}. It should be mentioned that the PDFs signal around 40 Å is dominated by the pair distances arising from the electronic density of the inorganic core, whereas the intensity of the PDFs curve around 90 Å is dominated by the electronic density of the protein shell. Keeping in mind that the PDFs curves presented in Figure 2 were normalized using the area bellow the curve between 0 and 130 Å, the increase of the signal at 90 Å reflects the fact that a reduction of the core should be accompanied by the relative increase (because of the normalization) of the, otherwise low, shell signal. As previously stated, two possible iron release mechanisms can be proposed. Either iron atoms are reduced and extracted from the surface of the particle as can be expected for a compact defect-free particle or the atoms are extracted from within as expected for defective particles. Both mechanisms have well-defined signatures in the PDFs due to their different effects on the core structure. Whereas removal from the core surface produces a nucleus with a smaller size but constant excess electron density, depletion of occluded iron reduces the excess electron density of the core but keeps its size almost unchanged.

To obtain a deeper understanding of the structural aspects of the iron release mechanism, a low-resolution bead model of Ft_{2200}, Ft_{1200}, and Ft_{500} was produced using the simulated annealing method implemented in the program DAMMIN.[12] From the structural file produced by DAMINN, the center of mass of the particle was determined and the bead-counting histogram was calculated for each structure.

Figure 3 shows the normalized bead count histograms for Ft_{2200}, Ft_{1200}, and Ft_{500}, respectively. The vertical line indicates the (nominal) position for the inner ($R \approx 40$ Å) radius of the apoferritin shell. Red bars in the histogram represent the bead count for the inorganic oxide core ($R < 40$ Å), and green bars correspond to the bead count for the protein shell ($R > 40$ Å). A close inspection of the histograms in Figure 3 suggests the existence of holes inside the inorganic core. The release of iron from Ft_{2200} to Ft_{1200} mostly induces a reduction of the core density. The external core radius remains unchanged and the "internal core hole" slightly increases suggesting that the reductive demineralization does not proceed from the core surface but from within the particle. Further release of iron from Ft_{1200} to Ft_{500} proceeds in a similar fashion, although in this case an increase in the inner hole and a retreat of the outer surface of the core is also apparent, suggesting that both mechanisms (removal of iron from surface and from cavity) may be operative, which would explain the small variation in particle size, (5.9 to 5.7 nm) observed by TEM (Figure 1).

XANES Study. X-ray Absorption Spectroscopy (XAS) is a valuable tool for studying the electronic structure and local environment of specific atoms within a molecule or solid. The region extending up to ~100 eV above the absorption threshold, usually called XANES, is dominated by multiple scattering processes between the photoelectron and its atomic environment and electronic transitions between the core level and empty bound states. In previous DXAS-XANES studies, Theil et al.[13] determined the rate of iron reduction in horse spleen ferritin and postulated that the ferritin core had a heterogeneous chemical and crystal structure. Recently, Quintana et al.[4,6] confirmed the polyphasic nature of the ferritin core. The aim in the present study was to construct a model of the phase distribution in the ferritin core using the highly sensitive XANES technique.

XANES on Ft_{200}, Ft_{500}, Ft_{1200}, and Ft_{2200} as well as those of the reference compounds ferrihydrite, magnetite, and hematite were measured under the same experimental conditions. The resulting spectra were used for linear combination fits (using the procedure implemented in the program ATHENA from the

(10) Gider, S.; Awschalom, D. D.; Douglas, T.; Mann, S.; Chaparala, M. *Science* **1995**, *268*, 77–80.
(11) Liu, G.; Debnath, S.; Paul, K. W.; Han, W.; Hausner, D. B.; Hosein, H.-A.; Michel, F. M.; Parise, J. B.; Sparks, D. L.; Strongin, D. R. *Langmuir* **2006**, *22*, 9313–9321.
(12) Svergun, D. I. *Biophys. J.* **1999**, *76*, 2879–2886.
(13) Joo, M.-S.; Tourillon, G.; Sayers, D. E.; Theil, E. C. *Biometals* **1990**, *3*, 171–175.

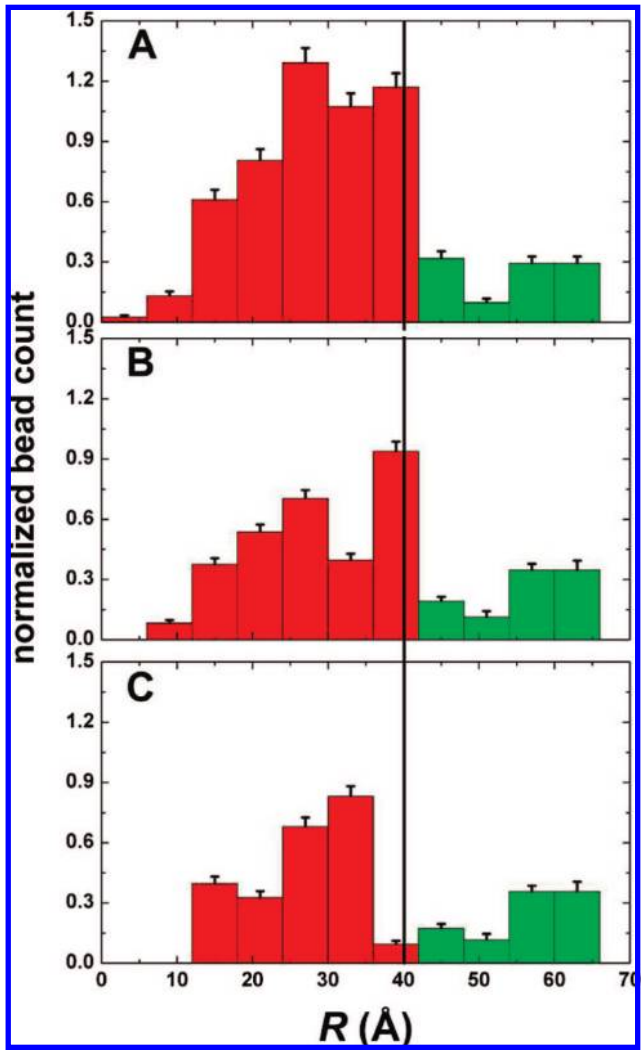

Figure 3. Normalized bead-count-histograms constructed from low resolution models of Ft_{2200} (panel A), Ft_{1200} (panel B), and Ft_{500} (panel C) obtained from SAXS experiments using the DAMMIN program (see text). Green bars correspond to the volume expected to be occupied by the protein shell (R > 40 Å), and red bars (R < 40 Å) correspond to the volume expected to be occupied by the inorganic core.

IFFEFIT package, between −20 and +80 eV around the absorption threshold; please see Supporting Information) to obtain the fraction of each iron oxide phase present in every ferritin sample. Figure 4 shows the fraction distribution in each sample for different degrees of iron removal. Error bars for the populations in Figure 4 were obtained measuring five independent spectra for each iron content and averaging the populations obtained for each independent spectrum. As iron was removed, the relative amount of magnetite (red) rose steadily from ∼20% to ∼70% and the percentage of ferrihydrite (yellow) fell from ∼60% to ∼20%. These results confirm the heterogeneous structure of the ferritin core.

Taken together, TEM, SAXS, and XANES findings suggest a ferrihydrite-enriched core with a surface predominantly formed by magnetite (Figure 5). Moreover, with this core−shell structure in mind, the present comparative study of ferritin cores with gradual reduction of their iron contents indicates that, as expected, the ferrihydrite phase is more labile to chemical reduction and mobilization compared with the magnetite phase.

EELS Study. Spatially resolved EELS was used to probe the iron oxidation state distribution across individual nanoparticles. In

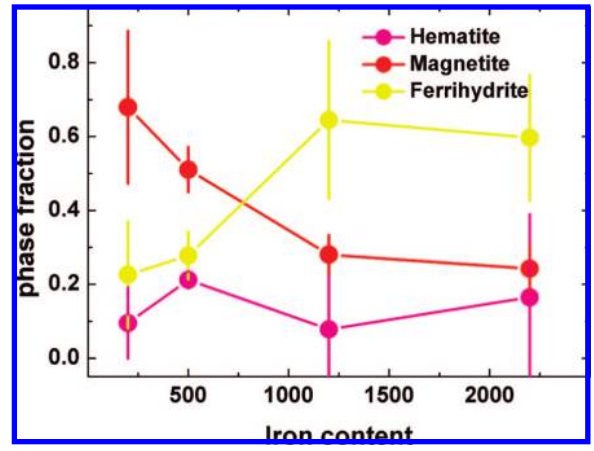

Figure 4. Phase distribution for ferritin samples with different iron content (200−2200 atoms) obtained from XANES experiments (see text). Purple (hematite), red (magnetite), and yellow (ferrihydrite).

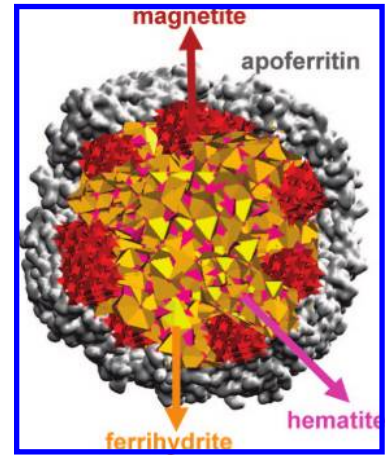

Figure 5. Schematic core−shelled ferritin iron core structure.

particular, a qualitative analysis of the $FeL_{2,3}$ edge fine structures allowed us to distinguish between iron(II) and iron(III).

We analyzed a series of nanoparticles corresponding to the sample Ft_{500} using the so-called Spectrum-Line (SL) technique. In this experimental approach, a collection of EEL spectra is sequentially acquired while a fine (usually in the order of a few angstroms) electron probe is scanned along a predefined path on the sample. In this study, 64 spectra were acquired with a 0.5 nm probe, a 0.4 nm step between spectra, an energy dispersion of 0.3 eV, and an acquisition time of 1 s per spectrum. These experimental conditions give access to energy and spatial resolutions of 0.5−0.7 eV and 0.5−1nm, respectively.

Figure 6 shows representative results of this EELS-SL study. The High Angle Dark Field (HADF) image shows one of the Ft_{500} particles (Figure 6b). The intensity line profile (Figure 6c) shows the HAADF variation along the particle, a signal that can be related to the projected sample mass. Figure 6a illustrates five spectra extracted from a spectrum line, with red points indicating the locations where the electron energy loss spectra were acquired. Positions 1 and 5 correspond to the surface of the particle, i.e., thinner regions, and positions 2, 3, and 4, to inner, bulk, sites. Figure 6a depicts the changes of the EEL spectra in the energy loss region of $FeL_{2,3}$ edges. Note how the position of the L_3 peak shifts slightly from the surface to the bulk. Thus, the peak is situated at 709.9 eV in spectra acquired at the surface (points 1 and 5) and at 710.5 eV in those recorded inside the particle (points 2−4). This change

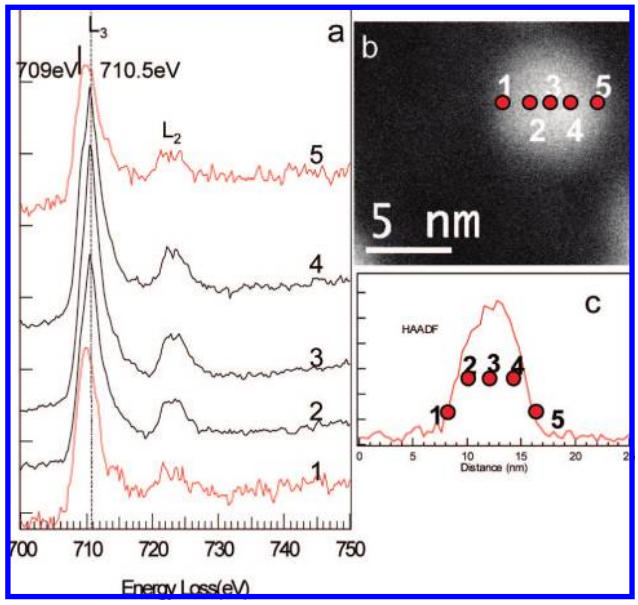

Figure 6. (a) EEL spectra in the energy loss region of $FeL_{2,3}$ edges. 1 and 5 correspond to the surface of the particle (the thinner regions), and 2, 3, and 4, to inner bulk sites. (b) A representative Ft_{500} particle (red points mark the locations where the electron energy loss spectra were acquired). (c) Intensity line profile variation along the particle shown in image b.

in the fine structure of the spectra correlates with a change in the oxidation state of iron. According to Gloter et al.,[14] the L_3 line displays a maximum at 709 eV for iron(III) species, while a shift toward a high energy value (710.5 eV) is observed for iron species. Consequently, our EELS results clearly evidence the presence of a higher fraction of iron(II) species at the surface of the ferritin cores.

These results contrast with findings of previous electron nanodiffraction studies, which found no differences in structure at the surface of the ferritin core in comparison with bulk.[4] In this context, it should be noted that Cowley et al.[4] used commercial horse spleen, usually containing about 2000 Fe atoms, whereas we used a batch of horse spleen ferritins in which iron was gradually removed from 2200 to 200 iron atoms. The comparative structural study of these samples (Ft_{2200}, Ft_{1200}, Ft_{500}, and Ft_{200}) allowed us to gain an insight into differences between the core and shell ferritin structure. Specifically, the EELS study of Ft_{500} indicated the existence of an iron(II)-enriched shell, which would not be evident in a ferritin containing 2000 Fe atoms, in which the mixed iron(II)−iron(III) phase shows an appreciably lower percentage.

SQUID Magnetic Study. The presence of a polyphasic structure in the ferritin core is consistent with recently reported magnetic studies on native ferritin.[15] Changes in the composition of the ferritin iron mineral during iron removal, especially the increase in magnetite, would affect the magnetic properties due to the high spontaneous magnetization and low coercivity of magnetite. The iron core of native ferritin containing about 2200 Fe atoms is antiferromagnetic below 140 K but has a net magnetic moment arising from uncompensated iron spins, largely at the surface of the core.[7,16] This ferritin behaves as a superparamagnet above 20 K with a marked hysteresis loop of magnetization below this blocking temperature. The magnetic behavior of Ft_{200} (70% magnetite, 20% ferrihydrite, 10% hematite) was studied and compared with that of Ft_{2200} (60% ferrihydrite, 20% magnetite and 20% hematite). A marked contrast between Ft_{200} and Ft_{2200} is observed in the variation of the magnetization with field at low temperature (2 K) (figure 7). The Ft_{2200} has a magnetic behavior characteristic of an antiferromagnet as ferrihydrite, with high coercitivity and low spontaneous magnetization, while the Ft_{200} exhibits higher remanence and higher spontaneous magnetization values, more typical of a ferrimagnetic magnetite phase.

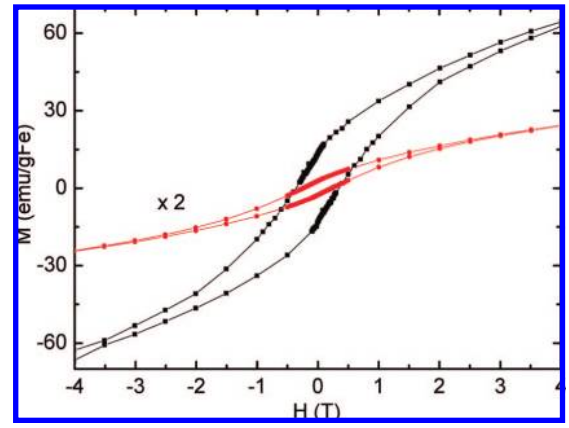

Figure 7. Hysteresis loop of magnetization per Fe atom of the lyophilized samples Ft_{2200} (red) and Ft_{200} (black). The magnetization values of Fe_{2200} were multiplied by 2 for clarity.

Iron Removing Study. The presence of mixed ferric−ferrous iron oxide phases, e.g., magnetite in the ferritin cores of patients with Alzheimer's disease, has been proposed as a cause of increased brain concentration of ferrous toxic iron. Although dissolution of iron from the ferritin core experimentally requires reduction of iron(III), the presence of iron(III)−iron(II) mineral phases does not ensure spontaneous ferrous delivery from the ferritin core. We studied the spontaneous release of iron(II) from the ferritin samples (Ft_{2200}, Ft_{1200}, Ft_{500}, and Ft_{200}) by incubating the ferritin with excess ferrozine at pH 7.4. Formation of the iron(II)−ferrozine complex was monitored by the appearance of its characteristic UV−visible band at 562 nm. No sample showed a significant increase in absorbance values at 562 nm. As an example, in the experiment with Ft_{500}, a concentration of 4×10^{-6} M was estimated from the absorbance value of 0.117 at 562 nm of the UV−visible spectrum and considering an extinction coefficient of 27 900 cm^{-1} M^{-1} for [Fe^{II}(ferrozine)$_3$] at 562 nm.[17] Based on the corresponding initial iron concentration in the ferritin solution, it was calculated that only 0.26% of the iron was removed from ferritin after 200 min. Close values (0.15−0.56%) were obtained for the remaining samples. Therefore, it can be reported that ferritin does not spontaneously release iron, even in samples with a predominance of a mixed ferric−ferrous iron oxide phase, e.g., magnetite.

Conclusions

The results collectively demonstrate that the native ferritin iron core consists of a polyphasic structure (ferrihydrite, magnetite, hematite) and that the proportion of each phase is changed by gradual iron removal, since ferrihydrite is more

(14) (a) Gloter, A.; Douiri, A.; Tence, M.; Colliex, C. *Ultramicroscopy* **2003**, *96*, 385–400. (b) Gloter, A.; Zbinden, M.; Guyot, F.; Gaill, F.; Colliex, C. *Earth Planet. Sci. Lett.* **2004**, *222*, 947–957.
(15) Brem, F.; Stamm, G.; Hirt, A. M. *J. Appl. Phys.* **2006**, *99*, 123906.
(16) Barco, L. F.; Hernández, E.; Remiro, J. M.; Bartolomé, E.; Tejada, J. *Phys. Rev. B* **1999**, *59*, 11837.
(17) Linert, W.; Herlinger, E.; Jameson, R. F.; Kienzl, E.; Jellinger, K.; Youdim, M. B. H. *Biochim. Biophys. Acta* **1996**, *1316*, 160–168.

labile to chemical reduction and mobilization compared to the magnetite phase. For the first time, a ferrihydrite−magnetite core−shell model has been tested for the ferritin iron mineral by TEM, SAXS, XANES, EELS, and SQUID magnetic measurements. The core mainly corresponds to a ferrihydrite phase in ferritin with physiological values of 1000−2000 irons, while magnetite appears to be the predominant phase when ferritin iron content decreases below 500 Fe. Moreover, iron core size does not significantly vary with iron removal, because iron is removed from the more chemically labile ferrihydrite core, hollowing it out, rather than from the magnetite shell.

The core−shell structure, which determines variations in the properties (size, magnetism, NMR relaxometry, etc.) of ferritin cores with gradual iron removal, can be produced by the chemical procedure used to prepare the ferritin batch. Iron(III) is reduced to iron(II) in the core and then leaves the ferritin cavity and is trapped by 2,2′-bipyridyl. Some of the as-formed iron(II) may be retained in the ferritin cavity, as reported by Watt et al.,[18] or some that is not complexed out of the cavity can again penetrate into and make contact and react with ferrihydrite to produce magnetite at the core surface. In this respect, it is important to note that ferrihydrite is a highly active mineral and known to be a precursor of more crystalline minerals as hematite.[19] A complete study of iron removal from ferritin in the absence of an iron(II) chelating ligand is in progress to demonstrate this hypothesis.

If magnetite is related to the free iron(II), the presence of magnetite in patients with Alzheimer's disease would not be a cause but a consequence of anomalies in the ferritin iron removal process. In the present paper, we have demonstrated that the presence of magnetite is not a source of free toxic iron(II).

Experimental Section

Preparation of Ferritin Samples. Horse spleen ferritin (lot 083K7051) was obtained from Sigma-Aldrich and exhaustively dialyzed against mill-Q water using a Spectra/Por Float-A-Lyzer with a molecular weight cutoff (MWCO) of 300 000 Da before use. The ferritin samples were prepared by partial core reduction of the commercially available ferritin (Ft_{2200}), using controlled thioglycolic acid/sodium acetate amount and reaction time in presence of 2,2′-bipyridyl (0.3 M).[7] After treatment, ferritin solutions were exhaustively dialyzed for 4 days at 4 °C with several changes of milli-Q water.

Atomic absorption analysis of the ferritin samples directly yielded iron concentrations, and apoferritin concentrations were determined on fully demetallated samples by a Lowry total protein micromethod assay (Sigma diagnostic) and confirmed by UV−visible absorbance at 280 nm ($\epsilon^{280} = 468\,000\ cm^{-1}\ M^{-1}$). An iron/apoferritin ratio of 2200, 1200, 500, and 200 was obtained for the respective ferritin samples Ft_{2200}, Ft_{1200}, Ft_{500}, and Ft_{200}. Note that the apoferritin concentration remains unaltered after iron removal.

Iron-Release Assays. Ferritin (2 mL, 38 mg/mL) in 0.15 M NaCl was incubated at room temperature with ferrozine (3-(2-pyridyl)-5,6-bis(4phenyl-sulfonic acid)-1,2,4-triazine (2 mM) at pH 7.4 (0.1 M TRIS, 0.1 M NaCl). Experiments were carried out in aerobic conditions. Development of the iron(II)-ferrozine complex was monitored spectrophotometrically at 562 nm, using $\varepsilon^{562} = 27\,900\ cm^{-1}\ M^{-1}$. Twenty 10-min cycles were recorded in a Thermospectronic UV300 spectrophotometer against reference solutions containing appropriate amounts of buffer-saline and ferrozine. The iron released from ferritin was expressed as a percentage of the iron−ferrozine formed and the initial ferritin iron concentrations.

Electron Microscopic Study. Samples used for the transmission electronic microscopy (TEM) study were prepared by placing a drop onto a carbon-coated Cu grid and drying it in a glovebox. Electron micrographs were taken with a Philips CM-20 HR analytical electron microscope operating at 200 keV. Electron Energy-Loss Spectra (EELS) were recorded in the VG-HB501 dedicated STEM at Orsay, working at 100 kV and using a 15 mrad convergence semiangle and 24 mrad collection angle. The spectrum line (SL) mode was used: this approach consists in acquiring a series of 64 EELS spectra while a 0.5 nm beam with a current of 0.1−0.3 nA is scanned along the sample. The high angle, dark field, scattered intensity signal (HADF) was also simultaneously collected at each point within the scanned area. This approach allows correlating nanoanalytical and structural information of the region under study. The above-mentioned instrument allows the recording of electron energy loss spectra, with high signal-to-noise ratios, using acquisition times as small as 1 s on the $L_{2,3}$ Fe edge. This small total acquisition time avoids sample drift, which could eventually limit the spatial resolution of the measurements. At the same time, sample irradiation problems are also minimized under these conditions, thereby increasing the reliability of the analytical data. This method was applied to six particles, and a high reproducibility of EELS was found, indicating that the particles are homogeneous and ruling out a possible system in which apoferritin molecules mostly contain ferrihydrite and the others magnetite.

Magnetic Measurements. Magnetic susceptibility measurements were performed on lyophilized samples using a magnetometer (Quantum Design MPMS-XL-5) equipped with a SQUID sensor. Variable-temperature measurements were carried out in the temperature range 2−300 K.

SAXS Measurements. SAXS experiments were performed in the D11A-SAXS1 experimental station of the National Synchrotron Light Laboratory, Campinas, Brazil. All experiments were performed at constant temperature (22 °C) using a circulating water bath. The incident wavelength was set at 1.448 Å, and the sample-to-detector distance, at 1066 mm. The scattering pattern was detected using a gas-filled 1D detector. Each spectrum was obtained as the average of at least five independent spectra. Corrections for beam intensity, sample absorption, and buffer scattering were performed following standard procedures. The Pair Distribution Function (PDF) was extracted from the scattering profiles using the regularized Fourier Transform method implemented in the GNOM 4.51 program.[20]

XAS Measurements. X-ray Absorption Spectroscopy (XAS) is a valuable tool for the study of the electronic structure and local environment of specific atoms within a molecule, cluster, or solid. The region extending up to ∼100 eV above the absorption threshold, usually called XANES, is dominated by multiple scattering processes between the photoelectron and its atomic environment and electronic transitions between the core level and empty bound states. XAS measurements were performed in the D04B-XAFS1 experimental station of the National Synchrotron Light Laboratory, Campinas, Brazil.

The sample was prepared by mixing a 2 mg ferritin sample with 10−15 mg of boron nitride. After gentle and careful mixing, the sample was compacted to less than 1 mm.

The average iron concentration within the sample was calculated to be 0.1−0.2 g cm^{-3}. Samples were exposed for ∼30 min to the radiation beam, and typically, five independent frames were acquired for each sample. Visual inspection of first and last data frames ruled out the occurrence of radiation damage. The experiments were performed using a Si220 channel cut monochromator with a calculated energy resolution (at 7112 eV including experimental resolution and natural line width) of ∼1.5 eV. All experiments were performed at room temperature (∼22 °C) in transmis-

(18) Jacobs, D. L.; Watt, G. D.; Frankel, R. B.; Papaefthymiou, G. C. *Biochemistry* **1989**, *28*, 1650–5.
(19) Schwertmann, U.; Friedl, J.; Stanjek, H. *J. Colloid Interface Sci.* **1999**, *209*, 215–223.
(20) Svergun, D. *J. Appl. Crystallogr.* **1992**, *25*, 495–503.

sion mode using a metallic iron foil for energy calibration and individual spectra alignment. Reference samples were prepared by deposition onto 5 μm cellulose filtering membranes to achieve uniform sample width. All chemicals were purchased from Aldrich and used without further purification or prepared (ferrihydrite) following the procedures described in the literature.[21] Data reduction and analysis were performed using the IFEFFIT package.[22]

Acknowledgment. We are grateful to the MEC (project CTQ2006-02840) and Junta de Andalucía (Proyecto Excelencia FQM-02525) for financial support. N.G. and S.T. thank the MEC for a research contract (Ramón y Cajal program). The authors acknowledge financial support from the France-Spain Bilateral Project HF2005-0046 and the EU under the Framework 6 program under a contract for an Integrated Infrastructure Initiative, Ref. 026019 ESTEEM. M.C. is a staff member of CONICET, Argentina and professor at the Universidad Nacional del Noroeste de Buenos Aires, Argentina. The authors also acknowledge Laboratorio Nacional de Luz Sincrotron, Campinas, Brazil, for partial financial support (Projects D11A-SAXS1-4172 and D04B-XAFS1-4581). M.C. acknowledges partial financial support from CONICET, Argentina.

(21) Towe, K. M.; Bradley, W. F. *J. Colloid Interface Sci.* **1967**, *24*, 384–392.
(22) Newville, M. *J. Synchrotron. Radiat.* **2001**, *8*, 322–324.

Supporting Information Available: Figure SM1: Stained (uranyl acetate) TEM image of the ferritin sample containing 500 Fe atoms. Figure SM2: (Upper panel) Average XANES spectra obtained for different iron contents (see the legend inside the figure); (Lower panel) residual of the least-squares fit (black, Ft_{2200}; red, Ft_{1200}; green, Ft_{500}; blue, Ft_{200}). Figure SM3: XANES data for the reference compounds (ferrihydrite, magnetite, and hematite). This material is available free of charge via the Internet at http://pubs.acs.org.

JA800492Z